sustainability

Article

Strategy for Locating People to Reduce the Transmission of COVID-19 Using Different Interference Measures

Brenda Valenzuela-Fonseca [1], Rodrigo Linfati [2] and John Willmer Escobar [3,*]

[1] School of Industrial Engineering, Universidad del Bío-Bío, Concepción 4030000, Chile; brenda.valenzuela1601@alumnos.ubiobio.cl
[2] Department of Industrial Engineering, Universidad del Bío-Bío, Concepción 4030000, Chile; rlinfati@ubiobio.cl
[3] Department of Accounting and Finance, Universidad del Valle, Cali 760001, Colombia
* Correspondence: john.wilmer.escobar@correounivalle.edu.co

Abstract: COVID-19 is generally transmitted from person to person through small droplets of saliva emitted when talking, sneezing, coughing, or breathing. For this reason, social distancing and ventilation have been widely emphasized to control the pandemic. The spread of the virus has brought with it many challenges in locating people under distance constraints. The effects of wakes between turbines have been studied extensively in the literature on wind energy, and there are well-established interference models. Does this apply to the propagation functions of the virus? In this work, a parallel relationship between the two problems is proposed. A mixed-integer linear programming (MIP) model and a mixed-integer quadratic programming model (MIQP) are formulated to locate people to avoid the spread of COVID-19. Both models were constructed according to the distance constraints proposed by the World Health Organization and the interference functions representing the effects of wake between turbines. Extensive computational tests show that people should not be less than two meters apart, in agreement with the adapted Wells–Riley model, which indicates that 1.6 to 3.0 m (5.2 to 9.8 ft) is the safe social distance when considering the aerosol transmission of large droplets exhaled when speaking, while the distance can be up to 8.2 m (26 ft) if all the droplets in a calm air environment are taken into account.

Keywords: social distancing; interference functions; mathematical models; virus propagation; optimization

check for updates

Citation: Valenzuela-Fonseca, B.; Linfati, R.; Escobar, J.W. Strategy for Locating People to Reduce the Transmission of COVID-19 Using Different Interference Measures. *Sustainability* **2022**, *14*, 529. https://doi.org/10.3390/su14010529

Academic Editors: Miltiadis D. Lytras, Abdulrahman Housawi and Basim Alsaywid

Received: 22 October 2021
Accepted: 15 November 2021
Published: 4 January 2022

1. Introduction

After its discovery in China in December 2019, severe acute respiratory syndrome coronavirus 2 (SARS-CoV-2), which causes coronavirus disease 2019 (COVID-19), began to spread through most countries of the world, resulting in a large number of infections and deaths, and placing significant pressure on the health systems and governments of different countries, which, in many cases, did not have the resources or infrastructure to face the pandemic caused by the virus, as was the case in Chile [1,2]. The following sections describe the main components of the problem.

1.1. COVID-19 General Background

According to the information provided by the Ministry of Health, SARS-CoV-2 is a strain of the coronavirus family that had not been previously identified in humans. Coronaviruses cause diseases, ranging from the common cold to more complex diseases, such as severe acute respiratory failure [3,4]. According to World Health Organization (WHO) information, SARS-CoV-2 is transmitted mainly by person-to-person contact with an infected person (even if he or she does not present symptoms) [5]. COVID-19 is an infectious disease caused by SARS-CoV-2 [6]. The COVID-19 pandemic is considered the most significant current global threat because of the thousands of confirmed infections, accompanied by thousands of deaths, worldwide [7,8].

In COVID-19, the respiratory symptoms are very similar to those of influenza or a cold; therefore, it is difficult to distinguish this disease. In general, the virus begins with signs and symptoms similar to those of influenza: respiratory symptoms (similar to those of a cold), fever (high temperature), dry cough, shortness of breath, or fatigue, and respiratory difficulties [9]. In most cases, COVID-19 is mild, but it can be severe, and the virus can cause pneumonia or severe acute respiratory syndrome (SARS), a severe form of pneumonia, as well as kidney failure, and even death. Some infected people do not develop any symptoms in other cases, but they can still infect others. The average incubation period is 5 to 6 days, with a maximum of 14 days [10].

1.2. Virus Transmission Methods

Potentially, all people exposed to droplets in the environment or on contaminated surfaces can be infected [11]. Close contact (less than one meter) with a person with respiratory symptoms (coughing or sneezing) results in the risk of transmission because of the potential for the exposure of the mucous membranes (mouth and nose) or the conjunctiva (eyes) to respiratory droplets that can be infectious. In addition, indirect droplet transmission can occur through any inanimate object in the immediate environment of an infected person. Therefore, the COVID-19 virus can be spread by direct contact with an infected person, and indirectly by contact with surfaces in their immediate environment or objects they have used [12]. Jalabneh et al. [13] show evidence that several countries worldwide developed 17 mobile apps for tracing to control the COVID-19 pandemic during the selected time frame. The mobile apps were used to monitor self-isolated individuals, and identify individuals not wearing masks and whether they had close contact with an infected person, providing the exact time and place of the encounter, and the possible risk of infection. Moreover, Shams et al. [14] propose a web search engine based on the combination of natural language processing (NLP) and a machine learning algorithm. This web search engine enables SEMiNExt to read the user query from the search bar, classify the veracity of the query, and notify the authenticity of the query to the user, all in real-time, to prevent the spread of misinformation.

Transmission by droplets differs from airborne transmission (aerosols) since the latter takes place through droplet nuclei-containing microbes. The droplet nuclei have a smaller diameter than the saliva droplets and can remain in the air for prolonged periods and reach people more than 1 m away. Aerosol transmission occurs in specific environments, in particular, in indoor, crowded, and poorly ventilated spaces where infected people spend extended amounts of time with others, for example, restaurants, choir practices, gymnastics classes, nightclubs, offices, and places of worship [12].

1.3. Social Distancing

According to an analysis of people's behavior, when a person is sick because they have contracted any contagious virus, they automatically try not to come too close to others for fear of contagion. However, social distancing is more than staying away from sick people who cough or are not well. Social distancing means maintaining a safe distance from people who do not live in the same household [15].

Although social distancing is a new idea for the population, it is not a new concept for scientists who study the spread of diseases. They are adamant in stating that social distancing has a substantial impact on the spread of COVID-19. For this reason, scientists and authorities have widely emphasized social distancing and ventilation to control the ongoing pandemic in closed and open spaces. However, the foundations of these two strategies have been debated, especially concerning quantitative recommendations.

The answers to, "what is a safe distance?", and "what is sufficient ventilation?", are crucial for reopening companies and schools, but they depend on many medical, biological, and engineering factors. The Wells–Riley study, based on a perfect mixture for the prediction of the probability of infection related to the virus in the air, gave the underlying reasons for maintaining adequate social distances and the ventilation of spaces. The study indicated that 1.6 to 3.0 m (5.2 to 9.8 ft) is the safe social distance when considering the aerosol transmission of large droplets exhaled when speaking, while the distance can be up to 8.2 m (26 ft) if all saliva droplets are considered in a calm air environment. The projections that use the model illustrated that an increase in the social distance could significantly reduce the infection rate (20–40%) during the first 30 min, even with current ventilation practices; the minimum requirement for the ventilation or fresh air should vary with the distance condition, the exposure time, and the effectiveness of the air distribution systems [16].

The spread of the virus brought many challenges to locating people in facilities under distance constraints. In a study by Fischetti [17] a parallel approach between this problem and that of locating wind turbines in a coastal area was proposed, since both problems require the installation of "infrastructure" (turbines or people) in a given area, ensuring a minimum distance between them. Just as nearby people can infect each other, nearby turbines can "infect" each other, casting wind shadows (wake effects) that cause production losses. In both problems, it is desirable to minimize interference or infection. The effects of the wakes between turbines have been studied extensively in the literature on wind energy, and there are well-established interference models. However, the propagation functions of the virus are not the same. Therefore, we analyze alternative functions that can define the interference matrix (infection) already defined by Fischetti et al. [17] described in Appendix A.

Contribution. Given the nature of this problem, and the fact that it is the first time since the Spanish flu in 1918 that a situation of such magnitude has been faced, the proposal of this work is essential for optimizing social distancing between people, thereby reducing the risk of infection. The results of this paper are intended to be the beginning of future research on the issue of locating people to reduce the spread of the virus. This study is limited to theoretically analyzing the problem of distancing between people through three different scenarios, in which previous studies carried out by scientists were considered, taking into account how the virus is transmitted. This work can serve as a basis for the placement of people in schools, universities, parks, and other facilities that generate more significant risks of contagion.

It is necessary to mention that there are currently not enough mathematical models that determine the virus's behavior. This work evaluates mathematical functions of exposure to COVID-19 related to wind energy and interference models. That is, alternative functions are analyzed that serve to define an interference matrix, considering that people are dispersed in the available area, proposing, in addition, a minimum distance between them. In addition, the results obtained in this study can be helpful for future research with more complex considerations.

2. Proposed Methodology

As mentioned above, social distancing is a key method for reducing the spread of COVID-19. For this reason, it is necessary to formulate models that favor distancing between people and, thus, reduce the existing risk of infection. Each person in the space is assumed to be already infected; therefore, there is a percentage that represents the possibility of contagion if more people are located near them. The study was carried out in three different scenarios, with different geometric shapes, and how the model behaved in each situation was analyzed.

The development of a mathematical model to determine the appropriate distance between people is not complete because of the complexity of the virus propagation equations. For this reason, emphasis is placed only on the transmission of the virus and some interference functions seen in wind farms. Consequently, the results obtained face certain limitations, which can be addressed in future studies. However, the results can help to make decisions and reliably locate people, thereby reducing the risk of COVID-19 infection.

In the problem considered, we work with three different scenarios to model the virus's behavior in different situations. A mixed-integer quadratic programming (MIQP) model and a mixed-integer linear programming (MIP) model are considered; these models are analyzed to verify which of the two solves the problem of social distancing proposed in a shorter time for this research. The first scenario represents 10×9 m^2, and two situations are considered, the first with a separation between squares of 1×1 m^2, resulting in 90 nodes to analyze, and the second situation with 50×50 cm^2 squares, resulting in 360 nodes to analyze. The second scenario represents an 18×5 m^2 rectangle and, as in the previous case, the two instances, of 1×1 m^2 and 50×50 cm^2, considering 90 and 360 nodes, respectively, are analyzed. Finally, in the third scenario, a circle is analyzed. The intention was to make the circle with 90 squares so that it would be of a size similar to those of the previously proposed cases; however, finding the appropriate 90 squares is complicated; therefore, we work with a circle of radius, $\sqrt{26\ \text{m}^2}$, resulting in 89 nodes to analyze, with 1×1 m^2 squares.

This research assumes that all of the people who are located in the previously established space are infected with COVID-19; therefore, all are infectious to the people who are located around them. Likewise, we assume that these people are static in location. There is no movement of people since only an instant of time is analyzed; otherwise, this study would become more complex since we would have to analyze the displacement of people at different instants of time. In addition, only Interference Functions (A1)–(A3) are considered for the virus's behavior, without considering the types of ventilation to which they could be exposed, such as being in an outdoor space, or ventilation alone by windows, air conditioning, fans, among others.

2.1. Description of the MIQP Mathematical Model

The MIQP mathematical model considers the following parameters and sets:

Dist—Euclidean distance between nodes

P—Number of people in the space

N—Number of nodes in space

The decision variables defined for the model are as follows:

$$x_j = \begin{cases} 1 & \text{If there is a person located at the position } j \forall j \in N \\ 0 & \text{Otherwise} \end{cases}$$

y_j—Contagion rate of a person exposed to the virus at the position $j \forall j \in N$

$Infr_{ij}$—Interference that a person in Position i has with another in position $j \forall j \in N$

The objective function minimizes the sum of the contagion index among the people who are located in the space to be analyzed and is defined as follows:

$$Minimize\ Z: \sum_{j \in N} Y_j X_j \tag{1}$$

The constraints associated with the problem are:

$$\sum_{j \in N} X_j = P \tag{2}$$

$$Y_j = \sum_{i \in N} Infr_{ij} * X_i \qquad \forall\, j \in N \tag{3}$$

$$X_i + X_j \leq 1 \qquad \forall\, (i, j) \in P^2 \backslash dist_{ij} < diag \tag{4}$$

$$X_j \in \{0, 1\} \qquad \forall i \in P \tag{5}$$

$$Y_j \geq 0 \qquad \forall j \in P \tag{6}$$

The objective function represented in (1) considers the "wake effect" caused by turbines when they are located very close to each other. In this way, it is possible to model the behavior of the virus being studied since, in both cases, there is interference (or infection) that is expected to be minimized. According to (1), regardless of whether there is a person in the space, the variable, X_j, takes a value of one or zero; therefore, the objective function represents the sum of all the contagion indices that a person would potentially receive if all the people around them are infected with COVID-19.

Equation (2) establishes that, of all the possible places to locate people, a maximum of P (number of people to be located in the space) should be located, where there are N squares (nodes) corresponding to the total workspace. In the case of Constraint (3), it is established that the possibility of contagion of people considers the sum of all the interference, which corresponds to the functions provided by the study on locating wind turbines in a coastal area. This relationship is established in the sense that there are at least two people in the space. In particular, it requires the location of things in a certain area or space, ensuring a minimum distance between them, so as not to generate interference or infection. Constraint (4) prohibits the existence of a person in front, to the side, behind, and diagonally from another person; that is, it establishes a minimum distance so that no one is near other person. Note that the unknown diagonal, in this constraint, corresponds to the value taken by the diagonal; that is, in the case that the squares are sized 1×1 m^2, the diagonal takes an approximate value of $\sqrt{2} = 1.42$. On the other hand, in the case where the squares are sized 50×50 cm^2, the diagonal takes a value of $\sqrt{8} = 2.83$. Finally, Constraints (5) and (6) consider the nature of the variables.

2.2. Description of the MIP Mathematical Model

The MIP model works in a similar way to the MIQP model, adding a large M as a parameter, which transforms the quadratic model into a linear model, and is defined as:

$$LargeM = \sum_{i,j \in N} Infr_{ij} \tag{7}$$

The objective function seeks to minimize the sum of the contagion indices that a person receives when exposed to the virus and is represented as follows:

$$Minimize\ Z: \sum_{j \in N} Y_j \tag{8}$$

The constraints associated with the MIP model are:

$$\sum_{j \in N} X_j = P \tag{9}$$

$$\sum_{i \in N} Infr_{ij} * X_i \le Y_j + BigM * \left(1 - X_j\right) \qquad \forall\ j \in N \tag{10}$$

$$X_i + X_j \le 1 \qquad \forall\ (i,j) \in P^2 \backslash dist_{ij} < diag \tag{11}$$

$$X_j \in \{0,1\} \qquad \forall i \in P \tag{12}$$

$$Y_j \ge 0 \qquad \forall j \in P \tag{13}$$

In this case, the objective function represented in (8) establishes that the variable, Y_j, corresponds to the interference index of the interference functions (see Appendix A), which represent the "wake effect". Constraint (9) is the same as Constraint (2) of the MIQP model. Equation (10) operates in a way similar to that of Constraint (3), where it is established that the possibility of contagion must be greater than or equal to the sum of all the interference caused. Finally, Constraint (11) operates in the same way as Constraint (4). Finally, Constraints (12) and (13) consider the nature of the variables.

3. Computational Experiments

The implementation of the formulations was performed in AMPL using three different solvers: KNITRO (12.1.0); CPLEX (12.10.0.0); and Gurobi (9.0.2). The tests were performed on an i7-7700k CPU, with 32 GB RAM, and a Red Hat Enterprise Linux 8 operating system. The results for each of the scenarios are detailed below.

3.1. Scenario 1

This scenario considers the solution of the MIP and MIQP models without Constraints (4) and (11), respectively. Both models are solved with CPLEX and GUROBI.

3.1.1. Experiment 1

Figures 1 and 2 show the results of the computational times in the execution of the MIP and MIQP models, respectively. The computing times for the MIP with the two solvers are similar; however, the line representing the GUROBI solver is slightly further to the right than that of the CPLEX solver, which shows that the MIP model, GUROBI, finds the optimal solution in a shorter time. In the case of MIQP, the GUROBI solver needs a shorter solution time. Therefore, the results show that the GUROBI solver works better than the CPLEX solver for both the MIP and MIQP models.

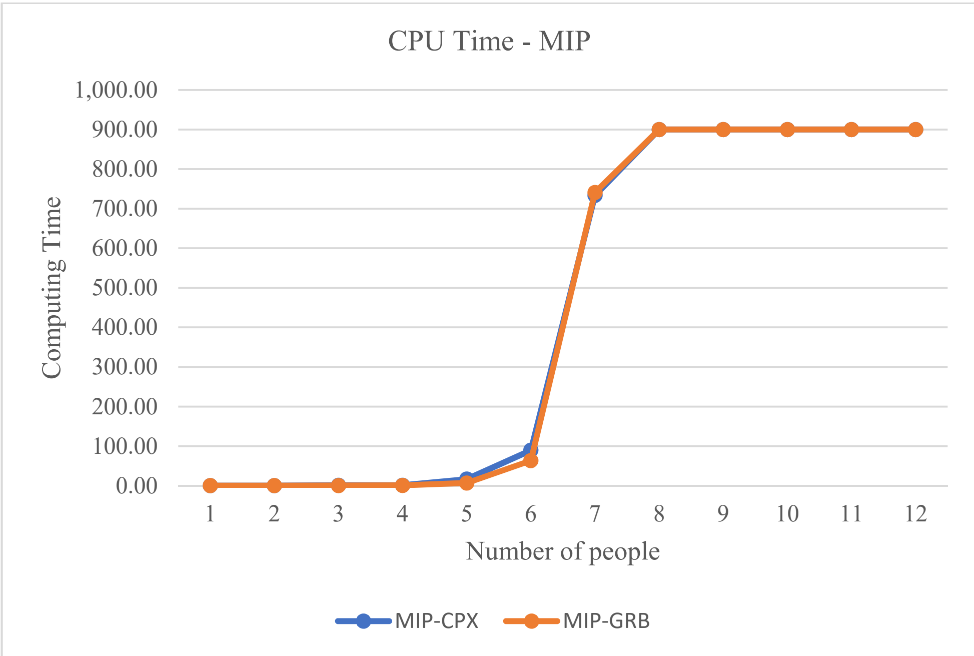

Figure 1. MIP solution time: Experiment 1. Source: Authors.

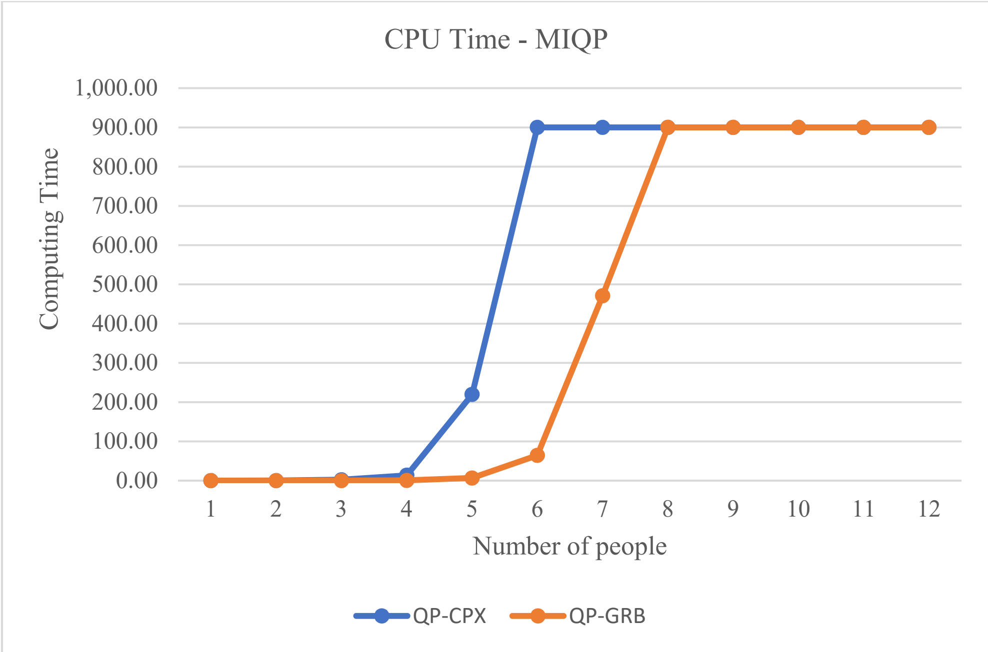

Figure 2. MIQP solution time: Experiment 1. Source: Authors.

3.1.2. Experiment 2

The computing times obtained with Constraints (4) and (11) in the MIQP and MIP models are shown in Figures 3 and 4, respectively.

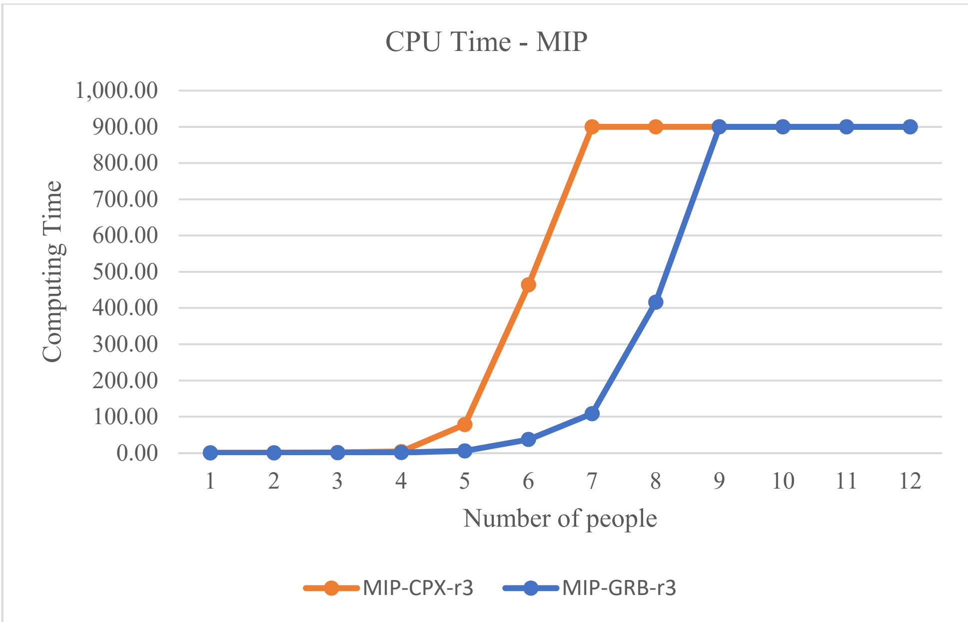

Figure 3. MIP model solution time: Experiment 2. Source: Authors.

When Constraint (11) is applied in the MIP model, the CPLEX solver begins to have a longer computing time than the GUROBI solver from the fifth person, and then from the ninth person, both solvers have the same time. For the MIQP model (Figure 4), the solvers function similarly to the previous case, where GUROBI is faster from five to nine people.

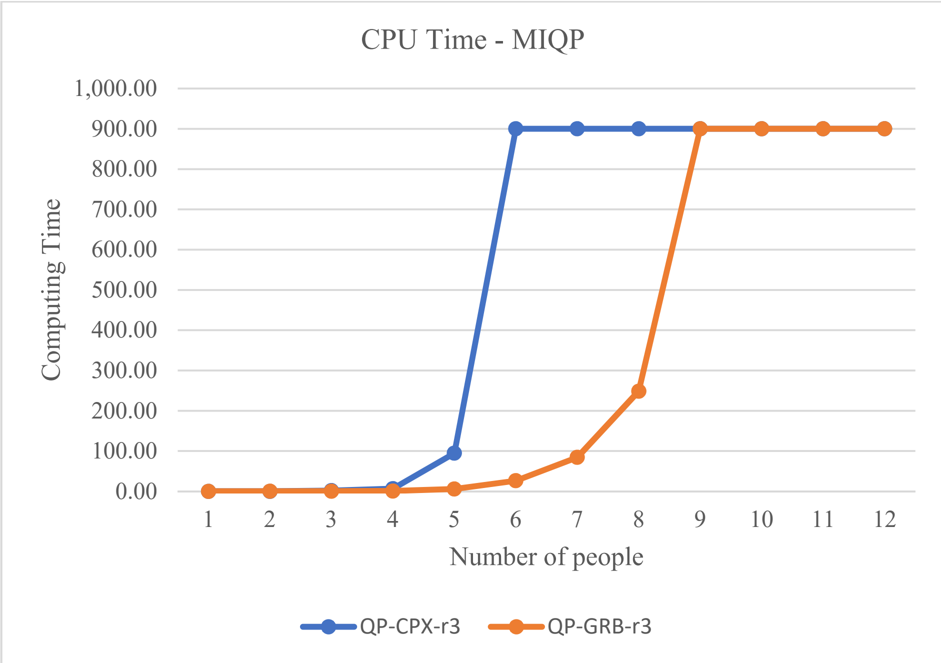

Figure 4. MIQP model solution time: Experiment 2. Source: Authors.

When Constraints (4) and (11) are applied in the MIQP and MIP models, the behavior of the computational time is similar to that obtained in Experiment 1. However, these constraints decrease the computational solution time.

3.2. Scenario 2

In this scenario, both models are evaluated on a rectangular shape (simulating a dressing room, soccer field, event hall, among others). In this way, we review any significant changes from Scenario 1.

3.2.1. Experiment 3

In this case, the MIP model is analyzed without using Constraint (11). Figure 5 shows that the best solver is GUROBI. In addition, in both cases, the MIP model works quickly in the beginning, but more slowly as the number of people in the space increases.

Figure 6 shows more clearly that the best solver for the MIQP model is GUROBI. In the case of CPLEX, the computing time begins to increase when the location of four people is evaluated and stabilizes when six people are located. On the other hand, the time used by GUROBI begins to increase when placing six people in the space and stabilizes when eight people are located. Although there is not much difference between the two models in terms of computing times, a slight variation can be observed when working with seven people, where the best model is MIQP solved with GUROBI.

3.2.2. Experiment 4

In this experiment, Constraints (4) and (11) are added to the MIP and MIQP models. Figure 7 shows that the MIP model is solved faster with the GUROBI solver. For the MIQP model, something similar happens with the MIP model (Figure 8).

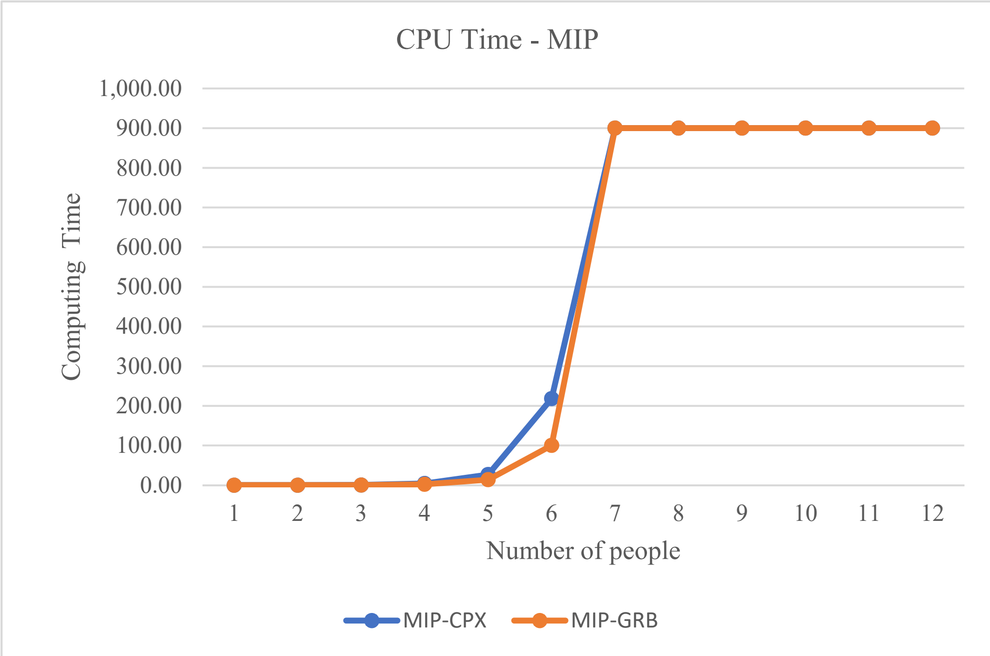

Figure 5. MIP solution time: Experiment 3. Source: Authors.

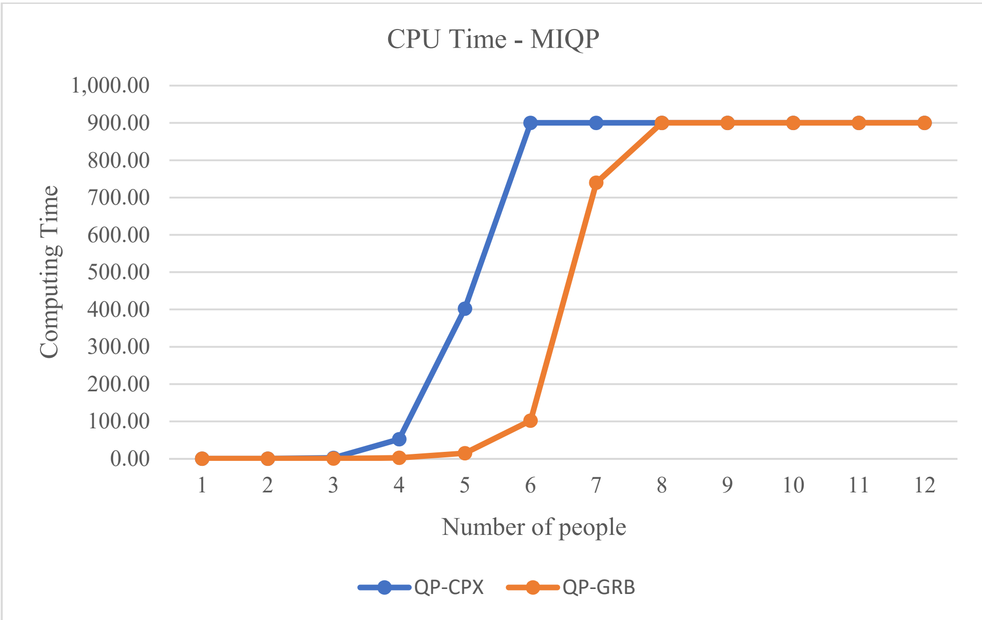

Figure 6. MIQP solution time: Experiment 3. Source: Authors.

There is little difference between the computing times of both models; however, in the MIQP model, the solution time shows a slight decrease in time when locating six people. For this reason, the MIQP model exhibits better behavior with the GUROBI solver when Constraint (4) is added.

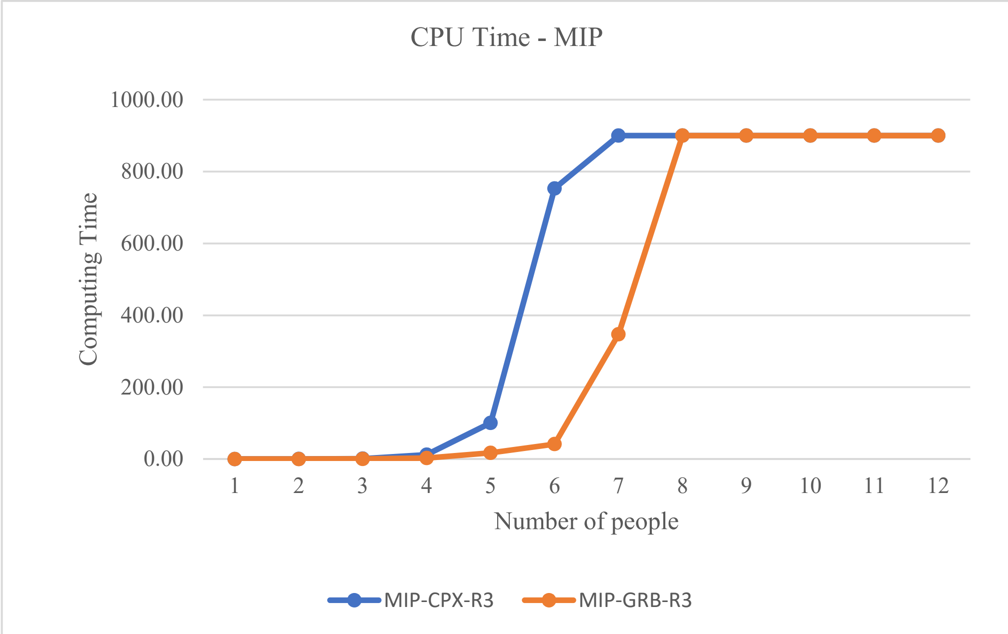

Figure 7. MIP model solution time: Experiment 4. Source: Authors.

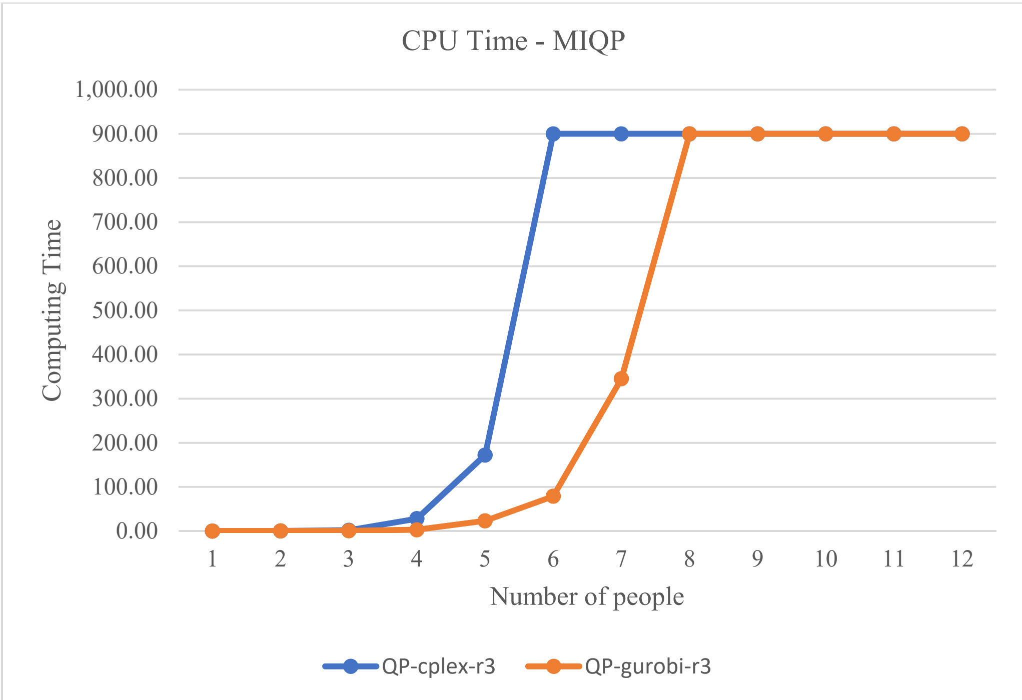

Figure 8. MIQP model solution time: Experiment 4. Source: Authors.

3.3. Scenario 3: Circle

In this scenario, the results obtained by working with a circular shape are evaluated (which can simulate a playground, rodeo, skating rink, among others.) In this way, the changes obtained in comparison with the figures presented previously can be observed. In this scenario, only the complete formulation of the models is analyzed because this decreases the computational time in the previous scenarios.

Experiment 5

As seen in Figure 9, the CPLEX solver has a longer computing time than the GUROBI solver once four people are located. As in the previous case, Figure 10 shows that the GUROBI solver needs a shorter computational time to find the optimal global solution with the MIQP.

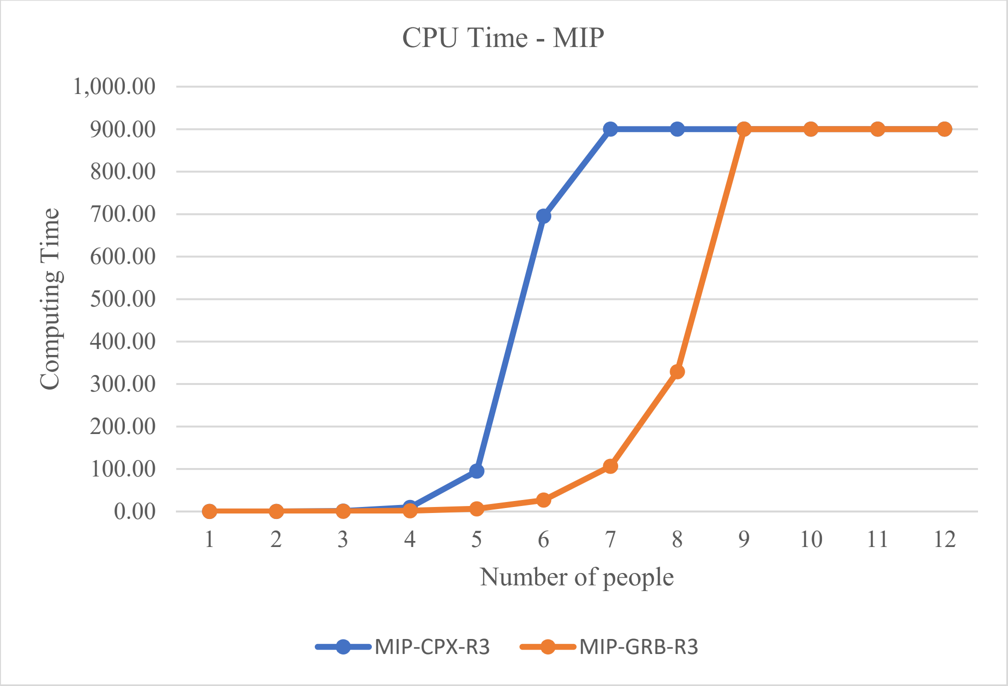

Figure 9. MIP model solution time: Experiment 5. Source: Authors.

A comparison of the models shows that both deliver similar computing times; however, the resolution time of the MIQP model is slightly to the right of that of the MIP model, which shows that the GUROBI solver more quickly solves the problem with the MIQP model. Therefore, the best model for analyzing a circular shape is the MIQP model using the GUROBI solver. Finally, the software, KNITRO, is easily trapped in local optima when solving the MIQP, so it is discarded as a possible solver for the problem considered.

3.4. Interference Function Results

After the computational times are analyzed, the results obtained by applying Interference Functions (A1) and (A2) are verified. Figure 11 shows a representation of the location of a person in space, applying both interference functions.

In the image on the left, it is observed that the virus has a more extraordinary trajectory when modeling the problem using the interference function (A2) since, as mentioned above, the function models the virus as if it traveled in the form of an aerosol. In contrast, in the image on the right, when a person is located in the first quadrant, the virus disappears when it reaches the third quadrant; that is, the virus has a maximum trajectory of approximately two meters (considering that each quadrant in the space measures 1×1). Therefore, when more people are placed in the space, a distance of two meters between people should be considered since, according to this function, there would be no probability of contagion. Next, four people are located within a given space, and the behavior of the interference functions analyzed is shown.

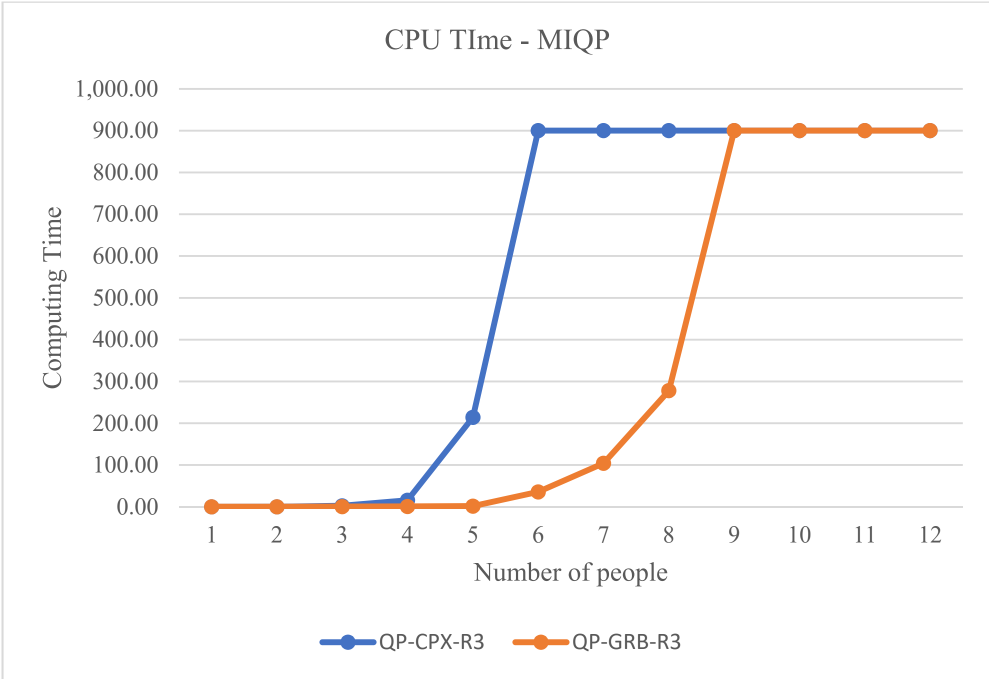

Figure 10. MIQP model solution time: Experiment 5. Source: Authors.

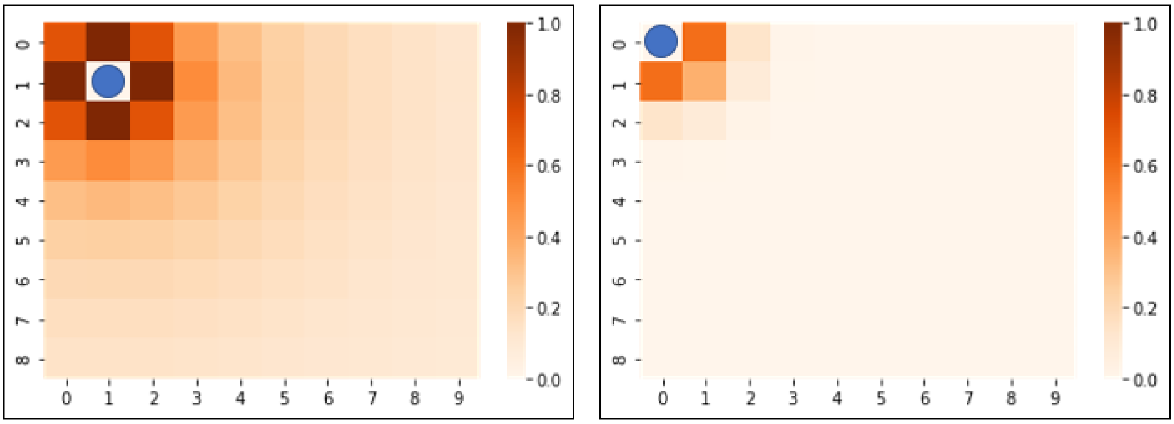

Figure 11. Representation of the interference functions when locating 1 person. Source: Authors.

Figure 12 of the image on the left shows how the model moves people as far apart as possible to reduce the risk of infection; however, the trajectory of the virus is much greater, so locating more people in the space becomes slightly more complex since, if more people are located in the space, they are already at risk of being infected. In the second case (image on the right), by applying the exponential interference function, the model separates the people in the space as much as possible, as in the previous case, so that there is no risk. However, there is still much space to continue locating people, and the risk of infection remains zero. Given the previous results, twelve people are placed within a space to verify the virus's behavior with a more significant number of people within the space, thereby comparing the two interference formulas considered.

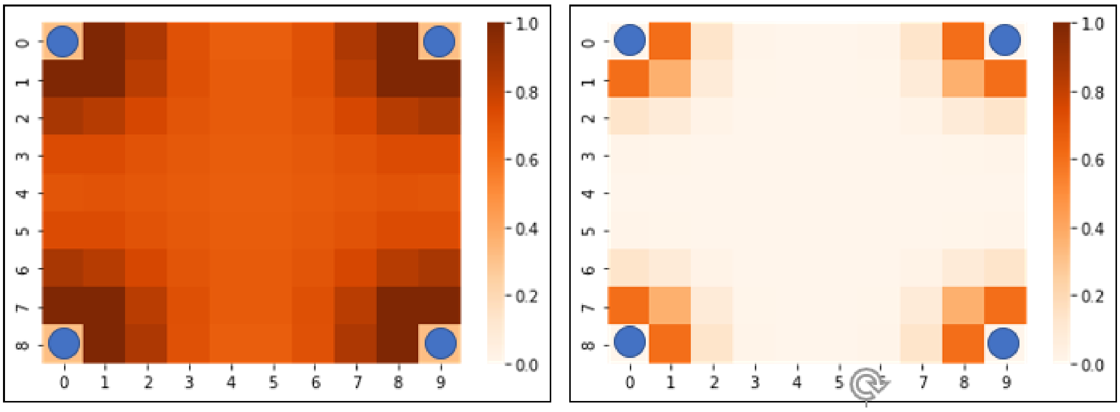

Figure 12. Representation of the interference functions when locating 4 people. Source: Authors.

Figure 13 (image on the left) shows the results obtained, in which the model separates the people as much as possible. However, when these people can no longer be separated further, the model groups them together so that the possibility of infection is minimal. Note that when trying to locate more people, all are at risk of contagion. In the second case (image on the right), the trajectory of the virus drops rapidly; therefore, the probability of contagion is zero if the minimum distance is respected, which makes it too simple a function from the point of view of the optimization since people can be separated enough (two quadrants) to avoid contagion. Once the results obtained by applying the different interference functions are known, a graph is prepared considering the indications that the Seremi de Salud is giving to compare the current situation in Chile, and the recommendations from the point of view of optimization.

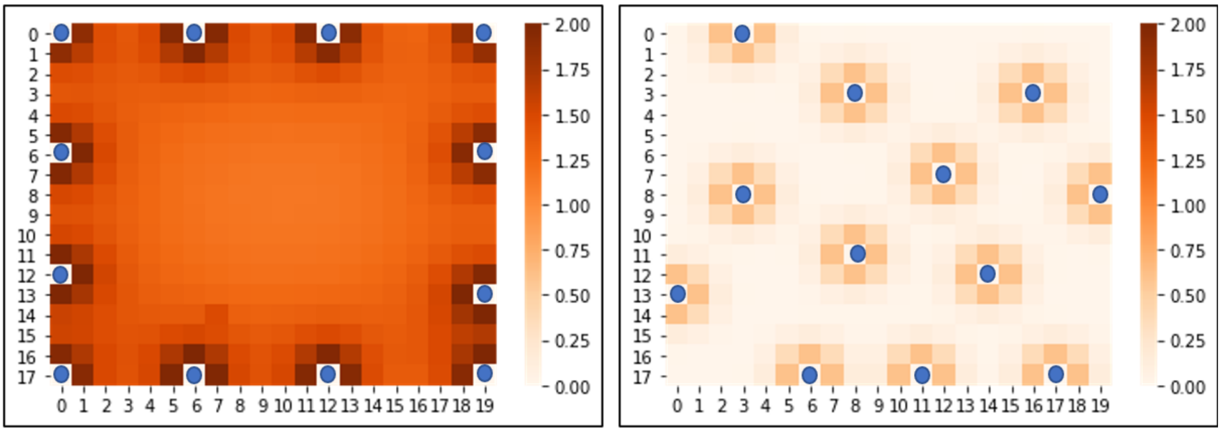

Figure 13. Representation of the interference functions when locating 12 people. Source: Authors.

The government of Chile assumes that the minimum distance between people should be greater than or equal to one meter; however, if this happens, Figure 14 shows that the risk of infection among people who are in the same space increases significantly since the probability of contagion is much higher. In addition, the measures provided by the government give very similar results as those when the first interference function is applied, since, in both cases, it is considered that the virus spreads in the form of drops that fall to the floor very quickly. According to the model adapted from Wells–Riley, 1.6 to 3.0 m (5.2 to 9.8 ft) is the safe social distance when considering the aerosol transmission of large droplets exhaled when speaking, while the distance can be up to 8.2 m (26 ft) if all drops in a calm air environment are taken into account [16]. Therefore, if these results are taken into account, the distancing measures taken by the Chilean government are far from correct [1].

Figure 15, presented below, shows how the virus spreads by droplets of saliva or in the form of an aerosol.

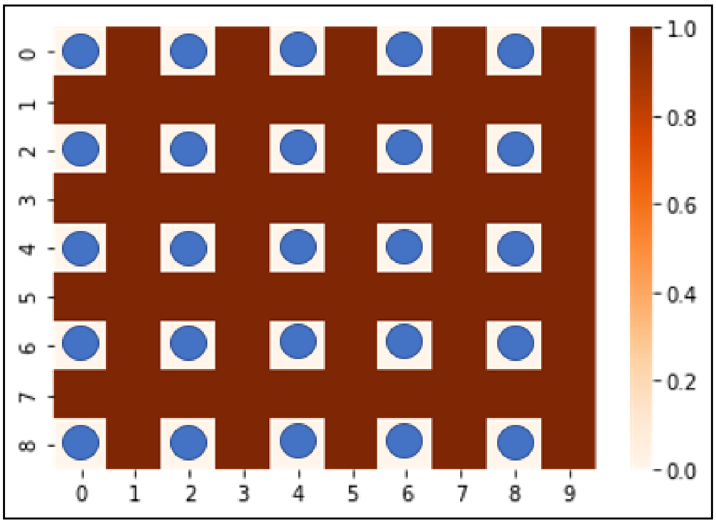

Figure 14. Indications given by the Seremi de Salud in Chile. Source: Authors.

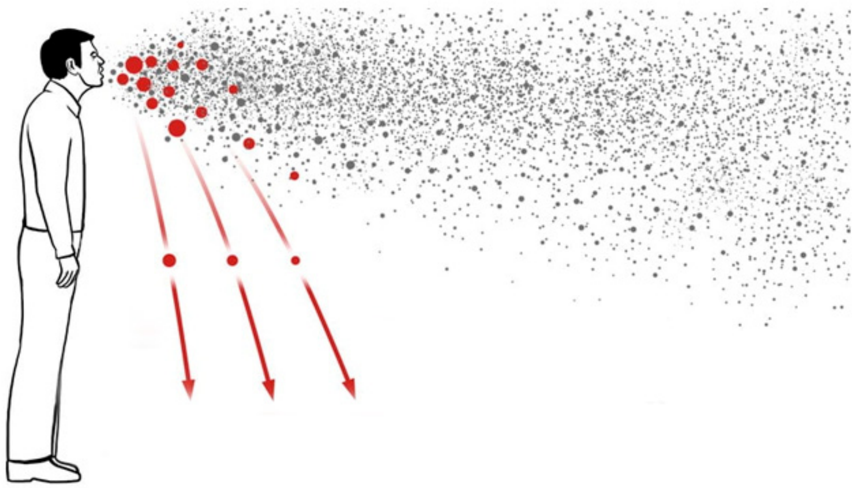

Figure 15. Transmission of the virus in the form of drops versus aerosol. Source: Authors.

3.5. Discussion Results

The saliva droplets (red circles) are large particles, falling rapidly to the floor in approximately two meters, which does not happen when the virus spreads in the form of an aerosol (black circles), since these particles are much smaller, causing the virus to spread to a much greater distance and to be in the air for a longer time. As mentioned above, this research is based on the assumption that all the people in a previously determined space could be infected with COVID-19. Additionally, it is assumed that these people are static in the place; that is, there is no movement of people in space since only an instant of time is analyzed; otherwise, the study would become even more complex since it would be necessary to analyze the displacement of people at different instants of time. Together, only the interference functions are considered in terms of the virus's behavior, without considering the types of ventilation in the space, such as ventilation in an open space, and ventilation only by windows, air conditioning, and fans.

There has been much talk about ventilation in closed spaces to control the pandemic since spaces that constantly move outside air are safer, replacing the contaminated air inside. Generally, outdoor air is pumped through heating systems, air conditioning, windows, and doors in commercial buildings, universities, companies, and homes. This air dilutes any contaminants, whether from viruses or something else, and reduces the exposure of any person inside. Each time a person exhales, carbon dioxide (CO-2) is released into the air. Given that COVID-19 is transmitted more frequently by breathing, coughing, or talking, CO-2 levels can be used to verify whether a room or space is filling with potentially infectious exhalations. The level of this component allows us to estimate whether enough fresh air is entering from the outside. Outside, CO-2 levels are above 400 particles per million (ppm). A well-ventilated room contains approximately 800 ppm CO-2. A slightly higher value would be a sign that the room might need more ventilation. Given that the coronavirus spreads through the air, the higher levels of CO-2 in a room probably mean a greater probability of transmission if an infected person is inside [18].

Note that solving this type of model is complex because of the large number of variables that must be considered in order to obtain a more detailed analysis, implying a weakness. On the other hand, it helps determine the best option for distributing people so that they run a lower risk of being infected by the COVID-19 virus. In the future, this would be an interesting topic to work on; however, it would be necessary to add more constraints, as is the cases of Constraints (4) and (11), which would serve to reduce computing times and help to find the optimal solution in the shortest possible time. In addition, an interference function can be used to model the spread of the virus along with specific directions, for example, because of the presence of air conditioning, fans, among others.

As a strength, the study carried out demonstrates that the use of mathematical optimization algorithms can improve the distribution in spaces, open or closed, decreasing the spread of the virus. This tool better manages the upcoming reopening of educational establishments, companies, and pubs, achieving the minimum risk of infection and, thus, helping people live with this new reality. Another approach toward the issue of COVID-19 infection is decreasing the time for detection of the virus. In Wuhan, Israel, Nebraska, and some localities in India, people have been tested through group testing (pool testing), which allows for the detection of large-scale infections in time to isolate them. This fact consists of grouping the samples of people. If this group test is positive, then each individual in the group is tested to determine who has the disease, while, in the opposite case, the individuals are not tested. In this way, if the groups to be tested are made up of five individuals, then pool testing uses six tests (if the group test is positive), and one test otherwise. In the first case, a more significant number of tests is used concerning the traditional testing methodology (six instead of five); however, in the second case, the number of tests to be used is significantly lower (from five to one) [19]. This methodology would alleviate the tremendous demand for exams, optimize the health system's resources, decongest laboratories worldwide, and would be interesting to research.

4. Conclusions and Future Work

In this paper, the optimal locations of people to maximize social distance and, thus, decrease the probability of contagion by COVID-19 are formulated mathematically. Regarding the solvers used, we concluded that KNITRO is not capable of finding a global optimum. In the computational implementation, the MIP and MIQP models are solved with CPLEX and GUROBI, and the solution times show that GUROBI works much better than CPLEX.

Likewise, we observed that, between the MIP and MIQP models, there is no considerable difference in the solution times of the problem. In addition, we can conclude that both solvers can find a global optimum with the MIQP model. When working with the heat map to model the results obtained by applying different interference functions, we confirm that the exponential function reflects the behavior of saliva droplets and that they vanish at approximately two meters; this does not happen with the other two interference functions, which represent the spread of the virus in the form of an aerosol.

In the course of this research, we can also observe that the measures taken by the Chilean government have not been adequate since, if the proposed models and the interference functions studied are applied, the majority of the people in a given space would be infected [1]. We propose using other interference measures and testing other scenarios related to other specific dimensions for future work. Moreover, as future research, we consider applying the same research to discuss its validity with regard to other respiratory diseases, especially influenza, by considering different interference metrics, which is very important and very topical for the Winter Stage.

Author Contributions: Conceptualization, B.V.-F., and R.L.; methodology, B.V.-F., R.L. and J.W.E.; software, B.V.-F.; validation, B.V.-F., R.L. and J.W.E.; formal analysis, R.L.; investigation, R.L.; resources, R.L.; data curation, B.V.-F., and R.L.; writing—original draft preparation, J.W.E.; writing—review and editing, J.W.E.; visualization, B.V.-F.; supervision, R.L. and J.W.E.; project administration, R.L. and J.W.E.; funding acquisition, R.L. All authors have read and agreed to the published version of the manuscript.

Funding: Not applicable.

Institutional Review Board Statement: Not applicable.

Informed Consent Statement: Not applicable.

Data Availability Statement: Not applicable.

Acknowledgments: This work has been partially supported by the research project, 2060222 IF/R and 2160277 GI/EF, from Universidad del Bio-Bio, and Universidad del Valle, Colombia. This support is gratefully acknowledged.

Conflicts of Interest: The authors declare no conflict of interest.

Appendix A

Consider that d_{ij} represents the Euclidean distance (in meters) between the positions, i and j, both in the available workspace. Alternative definitions for the interference, $Infr_{ij}$, that an installation (person) located in the position, i, has another person located in the position, j, are presented:

$$Infr_{ij} = e^{-\frac{d_{ij}^2}{2}} \tag{A1}$$

$$Infr_{ij} = \frac{1}{d_{ij}} \tag{A2}$$

$$Infr_{ij} = \frac{1}{d_{ij}^2} \tag{A3}$$

Definition (A1) assumes that the risk of infection can be modeled as a Gaussian function with Variance 1. The behavior of the saliva droplets can be observed in Figure A1, demonstrating that this function can be a realistic assumption for modeling the trajectory of saliva droplets, which are expected to decompose rapidly and fall within approximately two meters.

Figures A2 and A3 show the modeling of the virus's behavior according to Interference Functions (A2) and (A3). According to the information provided, Equations (A2) and (A3) assume, on the other hand, that an aerosolized virus spreads uniformly in spaces of one and two dimensions, respectively.

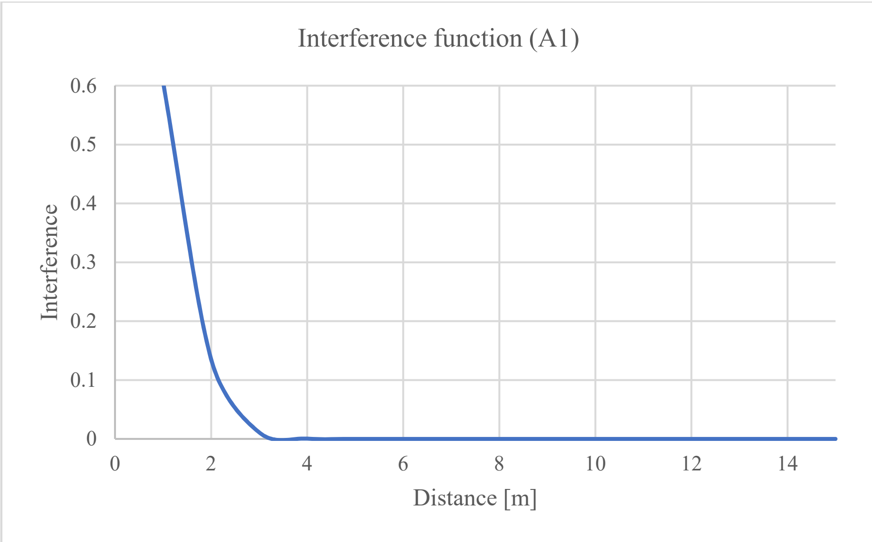

Figure A1. Interference function: Representation (A1). Source: Authors.

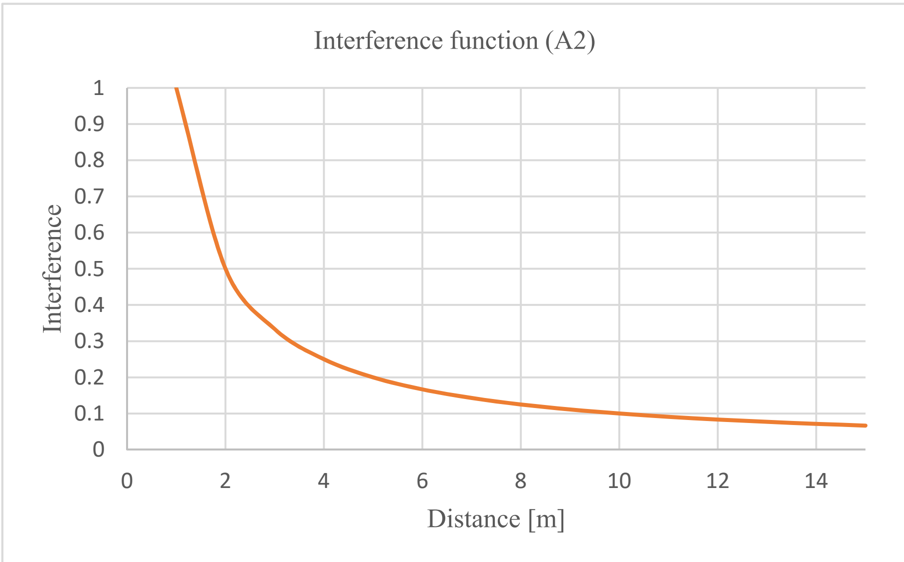

Figure A2. Representation of Interference Function (A2). Source: Authors.

Figure A4 clearly shows that Interference Function (A1) falls at a distance of two meters, confirming that this function simulates saliva droplets. In the case of Interference Function (A2), the virus spreads like an aerosol, which causes the probability of contagion in a given space to be even higher. In Interference Function (A3), the virus spreads in an aerosol; however, the interference drops off much faster than Interference Function (A2). Interference Function (A3) presents an analysis in two dimensions.

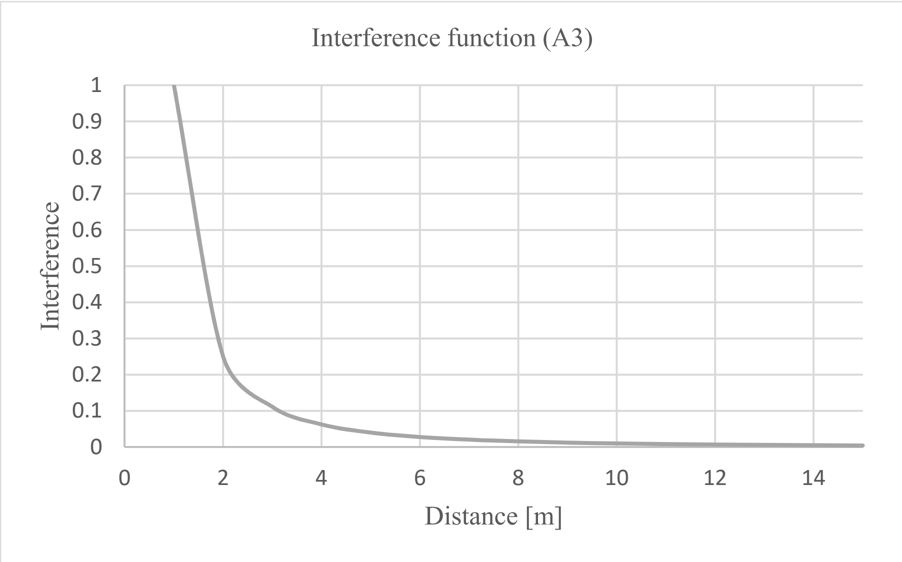

Figure A3. Representation of Interference Function (A3). Source: Authors.

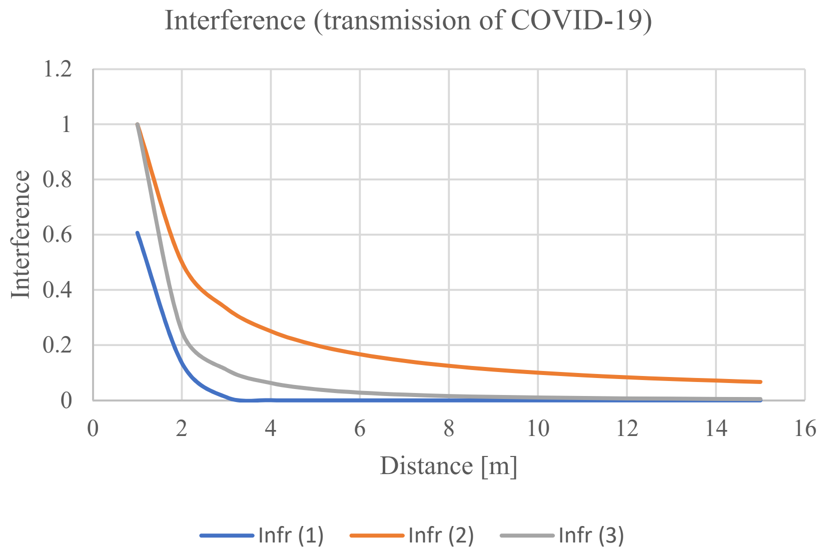

Figure A4. Comparison of interference functions. Source: Authors.

References

1. Caqueo-Urízar, A.; Urzúa, A.; Aragón-Caqueo, D.; Charles, C.H.; El-Khatib, Z.; Otu, A.; Yaya, S. Mental health and the COVID-19 pandemic in Chile. *Psychol. Trauma Theory Res. Pract. Policy* **2020**, *12*, 521–523. [CrossRef] [PubMed]
2. Sepulveda-Escobar, P.; Morrison, A. Online teaching placement during the COVID-19 pandemic in Chile: Challenges and opportunities. *Eur. J. Teach. Educ.* **2020**, *43*, 587–607. [CrossRef]
3. Wang, J.; Hajizadeh, N.; Moore, E.E.; McIntyre, R.C.; Moore, P.; Veress, L.A.; Yaffe, M.B.; Moore, H.B.; Barrett, C.D. Tissue plasminogen activator (tPA) treatment for COVID-19 associated acute respiratory distress syndrome (ARDS): A case series. *J. Thromb. Haemost.* **2020**, *18*, 1752–1755. [CrossRef]
4. Schenck, E.J.; Hoffman, K.; Goyal, P.; Choi, J.; Torres, L.; Rajwani, K.; Tam, C.W.; Ivascu, N.; Martinez, F.J.; Berlin, D.A. Respiratory Mechanics and Gas Exchange in COVID-19–associated Respiratory Failure. *Ann. Am. Thorac. Soc.* **2020**, *17*, 1158–1161. [CrossRef] [PubMed]
5. Ministerio de Salud. Minsal. 2020. Available online: minsal.cl/nuevo-coronavirus-2019-ncov/ (accessed on 7 October 2020).
6. Hu, B.; Guo, H.; Zhou, P.; Shi, Z.L. Characteristics of SARS-CoV-2 and COVID-19. *Nat. Rev. Microbiol.* **2021**, *19*, 141–154. [CrossRef] [PubMed]

7. Ndaïrou, F.; Area, I.; Nieto, J.J.; Torres, D.F. Mathematical modeling of COVID-19 transmission dynamics with a case study of Wuhan. *Chaos Solitons Fractals* **2020**, *135*, 1–6. [CrossRef] [PubMed]
8. Mansuri, F.M. Situation analysis and an insight into assessment of pandemic COVID-19. *J. Taibah Univ. Med. Sci.* **2020**, *15*, 85–86. [CrossRef] [PubMed]
9. Gautier, J.; Ravussin, Y. A New Symptom of COVID-19: Loss of Taste and Smell. *Obesity* **2020**, *28*, 848. [CrossRef]
10. Chen, H.; Ai, L.; Lu, H.; Li, H. Clinical and imaging features of COVID-19. *Radiol. Infect. Dis.* **2020**, *7*, 43–50. [CrossRef]
11. Solar, S.; Vial, P.; Rosas, R. Coronavirus Covid-19: Claves Para Entender la Enfermedad y Protegerse. Clínica Alemana. 2020. Available online: https://www.clinicaalemana.cl/coronavirus-covid19/coronavirus-claves-entender-enfermedad (accessed on 7 October 2020).
12. Organización Mundial de la Salud. *Vías de Transmisión del Virus del COVID-19: Repercusiones Para las Recomendaciones Relativas a las Precauciones en Materia de Prevención y Control de las Infecciones*; World Health Organization: Geneva, Switzerland, 2020.
13. Jalabneh, R.; Syed, H.Z.; Pillai, S.; Apu, E.H.; Hussein, M.R.; Kabir, R.; Arafat, S.M.Y.; Saxena, S.K. Use of mobile phone apps for contact tracing to control the COVID-19 pandemic: A literature review. In *Applications of Artificial Intelligence in COVID-19*; Comparative Law eJournal; 2021; pp. 389–404. Available online: https://papers.ssrn.com/sol3/papers.cfm?abstract_id=3641961 (accessed on 1 March 2021).
14. Shams, A.; Apu, E.H.; Rahman, A.; Raihan, S.; Siddika, N.; Preo, R.; Hussein, M.; Mostari, S.; Kabir, R. Web Search Engine Misinformation Notifier Extension (SEMiNExt): A Machine Learning Based Approach during COVID-19 Pandemic. *Healthcare* **2021**, *9*, 156. [CrossRef] [PubMed]
15. Lyness, D. TeensHealth. 2020. Available online: https://kidshealth.org/es/teens/coronavirus-calmesp.html#:~{}:text=%C2%BFQu%C3%A9%20es%20el%20distanciamiento%20social,6%20pies%20(2%20metros) (accessed on 13 November 2020).
16. Sun, C.; Zhai, Z. The efficacy of social distance and ventilation effectiveness in preventing COVID-19 transmission. *Sustain. Cities Soc.* **2020**, *62*, 102390. [CrossRef]
17. Fischetti, M.; Fischetti, M.; Stoustrup, J. Mathematical optimization for social distancing. *ResearchGate* **2020**, *20*. [CrossRef]
18. Daley, B. ¿Cómo Puedes Utilizar la Ventilación Para Prevenir la Propagación de COVID-19? The Conversation. 2020. Available online: https://theconversation.com/como-puedes-utilizar-la-ventilacion-para-prevenir-la-propagacion-de-covid-19-dentro-de-tu-casa-144456 (accessed on 25 February 2021).
19. Thraves, C.; Saure, D. COVID-19: Pool Testing, Hacer Más con Menos. CIPER. 2020. Available online: https://www.ciperchile.cl/2020/06/11/covid-19-pool-testing-hacer-mas-con-menos/ (accessed on 1 March 2021).